

# All-Photonic Link for High-Performance Antenna Arraying

S. Huang<sup>1</sup> and R. L. Tjoelker<sup>1</sup>

*A stabilized all-photonic link is described that significantly simplifies X-band (approximately 8 to 12.5 GHz) and Ka-band (approximately 18 to 40 GHz) signal transport for high-performance antenna array applications. A cost-effective, integrated fiber-optic calibration technology provides long-term phase stability in the actual link used for broadband signal transport. This should directly benefit antenna array downlink applications that require signal phase alignment at a central site in order to correlate received signals. It also provides direct benefit to antenna array uplink applications that require phase alignment of all transmitted signals at the receiving target. We report the general design concepts with applicability to downlink/uplink array designs and present initial phase sensitivity tests and stabilization results.*

## I. Introduction

For useful application of time and frequency metrology, it is essential that the signal distribution capability not degrade the reference source or transported data. For example, the Deep Space Network (DSN) frequency and timing subsystem (FTS) has several fiber-optic distribution capabilities to transport calibrated and stable atomic frequency standard and clock reference signals to users distributed up to 30 km from the reference source. Applications requiring multiple antennas, such as antenna arraying and connected-element interferometry, place significant demands on relative and temporal stability of parallel distribution links to or from each antenna.

NASA has recently undertaken an ambitious effort to develop an antenna array system with the capability to replace the current DSN. A preliminary downlink design envisions ~400 twelve-meter-diameter antennas per DSN site to detect signals at both X-band (approximately 8 to 12.5 GHz) and Ka-band (approximately 18 to 40 GHz). This requires signal phase alignment between all antennas to successfully correlate received signals. This provides a challenge for stable and efficient signal processing at each antenna front end, along each distribution link, and at the signal processing center.

The initial baseline array design [1] and the method used in a three-antenna-element breadboard array on the JPL Mesa is to downconvert the received signal at each antenna before transport to a central correlation site. This requires an X-band local oscillator (LO) signal be centrally synthesized and distributed to and returned from each antenna and a separate transport line to transmit the downconverted

---

<sup>1</sup>Tracking Systems and Applications Section.

The research described in this publication was carried out by the Jet Propulsion Laboratory, California Institute of Technology, under a contract with the National Aeronautics and Space Administration.

intermediate frequency (IF) signal back to the central processing center. Operationally, subsets of the antenna elements will be selectable and tunable to different bands in order to simultaneously track multiple missions. This requires the X-band LO distribution also have a complicated switching and fan-out multiplexing scheme. Varying phase perturbations (typically thermal or mechanical in origin) in each fiber-optic link and associated electronics must be accounted for in order to phase align received and transported signals for correlation. This is accommodated in the three-antenna-element breadboard array by loop back of the X-band signal from each antenna, an additional X-band photonic receiver, and precision phase monitoring of each link [2]. As this is performed in fibers parallel to the actual IF transport fiber, the monitored data provide only an approximation of the actual phase perturbations experienced by the transported downconverted signal.

In addition to primary signal transport, typically one or two lower performance links are required for each antenna for monitor and control functions. For an array involving  $\sim 400$  antennas per site, more than one thousand optical links will be operating between the antennas and the control center. Simplicity and low initial and life cycle costs are key requirements for the signal distribution design. The DSN FTS currently uses both open-loop and stabilized transport links to distribute stable reference signals to frequency and timing users. For the most demanding DSN application, long-term phase variations over a 16-km fiber-optic cable are measured and controlled to very high precision by the JPL-developed Stabilized Fiber Optic Distribution Assembly (SFODA) [3–5]. This capability transports stable 100-MHz reference and 4-GHz exciter signals from Signal Processing Center 10 (SPC 10) to Deep Space Station 25 (DSS 25) in support of the Cassini Radio Science Gravity Wave Experiment. This technology is large and not cost effective for mass production to support hundreds of antenna elements, as envisioned for the downlink array.

## II. All-Photonic Link Approach

The all-photonic link approach combines the benefits of active stabilization [3–5] with an antenna remoting architecture (e.g., see [6]), resulting in a dramatically simplified signal architecture. Photonic components, such as transmitters, receivers, and modulators with capability up to 1 GHz, are cost effective and widely available in the telecommunications industry. Photonic components with the capability for signal processing at X-band are more expensive, although the availability of cost effective components continues to improve. For the proposed DSN array, signals must be transported at X-band and Ka-band. Ka-band components are also now commercially available, with markets growing and prices falling.

Nevertheless, significant initial and life cycle savings can be realized by keeping part counts down and, where possible, by using lower-frequency components. A key feature of the all-photonic link design presented here is the integration of a low-cost transport fiber stabilization method operating at  $\sim 400$  MHz. A central high-power laser provides the light channel for several antennas, thus eliminating the need for expensive X- and Ka-band-capable transmitters in each antenna. In this approach, only an X- and Ka-band optical modulator is required at each antenna. Received X- and Ka-band signals are directly modulated and transported to the central processing facility for correlation. This eliminates the need for radio frequency (RF) downconversion, phase-locked loops (PLLs), multipliers, or a separate IF transmitter, and significantly reduces the complexity, part count, environmental control, and maintenance requirements at each antenna.

## III. All-Photonic Link Concept for Downlink Arrays

The system design for a downlink array capable of receiving X- and Ka-band signals and transporting them without perturbing phase is shown in Fig. 1. For the main downlink signal path, a high-power laser diode (HPLD) generates light that is distributed to several antennas through a  $1 \times N$  optical power divider. Each channel of light from the output of the  $1 \times N$  divider is fed to an individual antenna (by

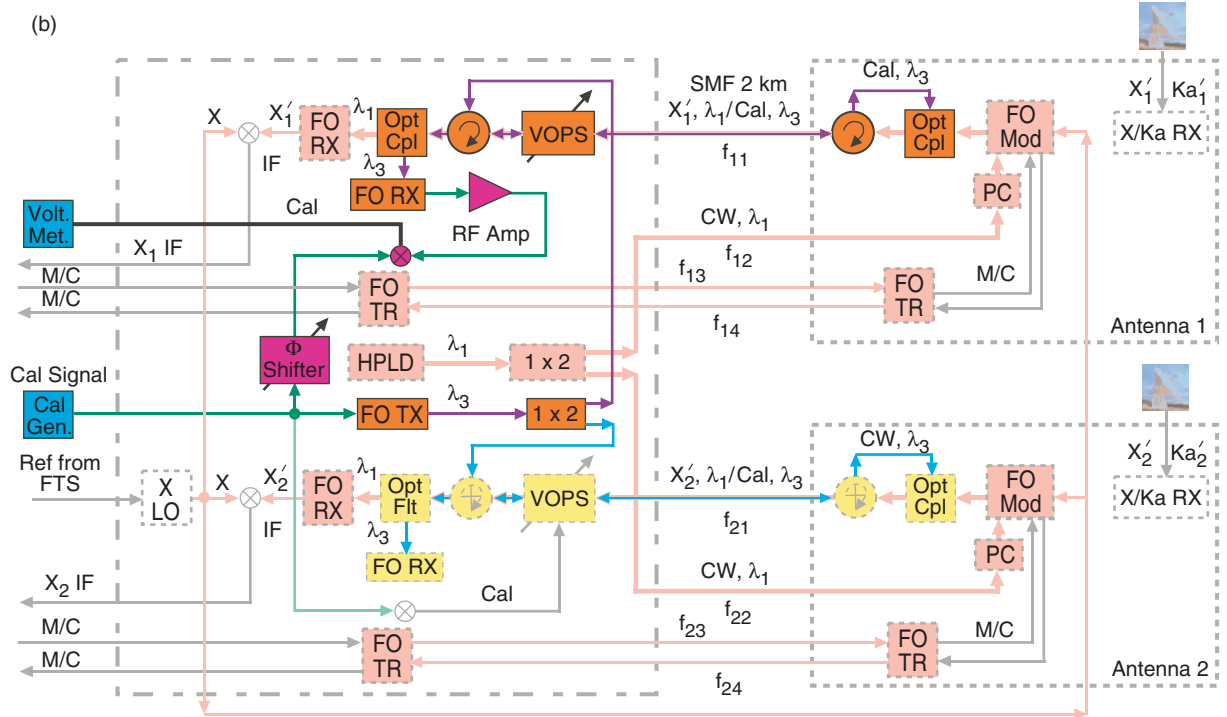
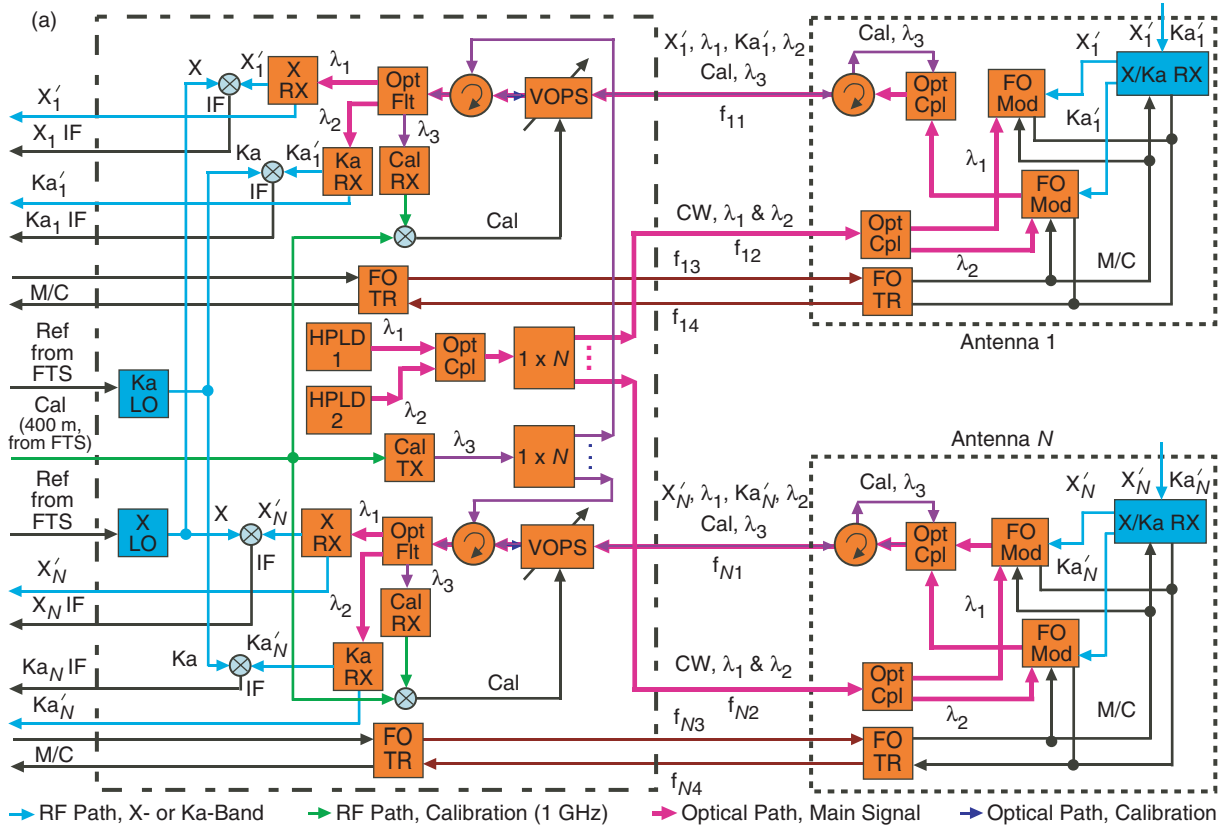


Fig. 1. Block diagrams: (a) conceptual design of the stabilized all-photonic link for an  $N$ -element antenna array capable of simultaneous reception of X- and Ka-band signals and (b) calibration channel test configuration through the RF and optical path of one array downlink element.

fiber  $f_{12}, f_{22}, \dots$ ), then passed through a polarization controller (PC) [shown in Fig. 1(b)] and launched into the fiber optical modulator (FO Mod). The PC may not be necessary for polarization insensitive modulators, which have recently become available. The received RF signal from the antenna front-end amplifier is used for driving the modulator at X-band, Ka-band, or both. Figure 1(a) shows the setup for both X-band and Ka-band operation. The output light (modulated by the received X-band signal) passes through an optical coupler (Opt Cpl), a circulator, and fiber  $f_{11}$  (or  $f_{21}, f_{31}, \dots$ ) back to the control center. At the control center, the signal light passes through a voltage-controlled optical phase shifter (VOPS), an optical circulator, and an optical filter to reach a fiber optical receiver (X-RX, Ka-RX, or Cal RX). The X-RX recovers the RF signal from the signal light ( $\lambda_1$ ) and provides it for further processing at the control center. Except for being at a slightly different optical wavelength,  $\lambda_2$ , the RF recovery for Ka-band signals is similar to the X-band system.

The optical signal path along the downlink fiber  $f_{11}$  (or  $f_{21}, f_{31}, \dots$ ) is stabilized to compensate for any phase change due to fiber-length fluctuations or other component sensitivity in the signal path. This phase compensation consists of a central, low-cost calibration laser transmitter (Cal TX) that is modulated by a fixed-frequency reference signal (currently 400 MHz in the breadboard). The calibration light ( $\lambda_3$ ) is sent out to each antenna and back through the signal fiber  $f_{11}$  [shown in Fig. 1(a)]. Approximately 99.9 percent of the critical signal path length is through fiber  $f_{11}$  ( $f_{N1}$ ). To stabilize the system, any phase-change variation is measured and compensated by comparing the phase of the reference calibration signal with the phase of the returned  $\lambda_3$  after RF demodulation. The error signal out of the phase comparator is then applied to a VOPS to compensate any phase variation over time.

The fibers  $f_{13}, f_{14}$  (and up to  $f_{n3}, f_{n4}$ ) are used for monitor and control (M/C) signals. The M/C is low frequency, and components are inexpensive. Fibers  $f_{13}$  and  $f_{14}$  (and up to  $f_{n4}$ ) are used for continuous wave (CW) light transmission and require no stabilization by the VOPS. The only photonic component in the signal path at the antenna is the modulator, which is passive and does not require sophisticated or expensive temperature control.

## IV. Component Performance Requirements

### A. High-Power Laser Diode

A high-power laser may be used for driving multiple antenna modulators. As Fig. 1(a) shows, the total insertion loss of the modulator, the optical coupler, two circulators, and the optical filter is approximately 11 dB. Assuming a laser power of +20 dBm (100 mW), the optical receiver requires a minimum input signal of -5 dBm and a system margin of 2 dB; then the total acceptable loss for the optical power divider is  $L_D = 20 - (-5) - 11 - 2 = 12$  dB. Therefore, a single high-power laser can support up to 16 antennas.

### B. Thermal Control Range

Temperature compensation is critical to achieve high-performance distribution, especially in open-loop systems. The maximum distance  $L$  between the antenna and the control center is expected to be about 1 km. Figure 2 shows ground temperature profiles as measured at the Goldstone Deep Space Communications Complex (GDSCC), located in the Mojave Desert [4]. Assuming the length of the signal fiber is 3 km and that  $\sim 98$  percent of the fiber cable is buried 1 meter underground, the temperature change on the fiber cable will be less than 0.5 deg C over 24 hours. This is  $\sim 1$  percent of the maximum surface temperature variation of  $\sim 40$  deg C at GDSCC.

Approximately 2 percent of the fiber (i.e., 60 m) may be more exposed (such as in cable vaults, antenna cable wraps, etc.) and may be subjected to direct air temperature variations. We assume a conservative worst case of  $\Delta T_{SF} = 50$  deg C for the surface temperature change and  $\Delta T_{UG} = 2.5$  deg C for the underground temperature change at 1-meter depth. The fiber thermal coefficient  $k$  is assumed to be the typical 7 ppm/deg C of a standard telecommunication fiber. (Lower thermal coefficient fiber

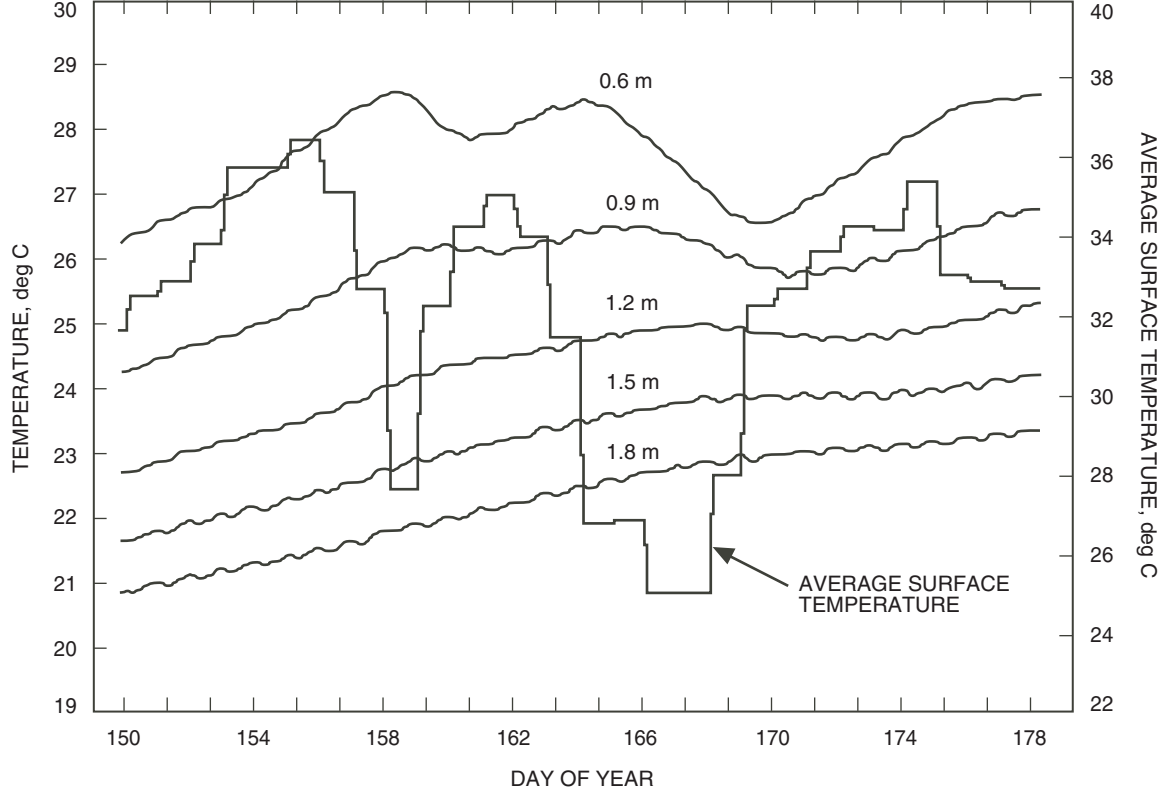


Fig. 2. Ground temperature profile of the GDSCC DSN site [4].

has been implemented in key short distance DSN links, although this special fiber is expensive and not easily available.) One meter of optical fiber is equivalent to  $\sim 5$  ns delay. Therefore, the total temperature-induced phase shift (delay change) may be expressed as  $D_T = D_{UG} + D_{SF}$ , where  $D_{UG}$  is the delay change caused by underground fiber and  $D_{SF}$  is that caused by fiber on the surface. Temperature-induced delay change ( $D$ ) can be calculated from the following equation:

$$D = L \times k \times \Delta T \times 5000 \text{ ps/m}$$

where  $L$  is the length of cable in meters,  $k$  is the thermal coefficient of the fiber (ppm/deg C), and  $\Delta T$  is the temperature change in deg C. Then,

$$D_{UG} = 2940 \text{ m} \times 7 \times 10^{-6} \times 2.5 \times 5000 \text{ ps/m} = 257 \text{ ps}$$

$$D_{SF} = 60 \text{ m} \times 7 \times 10^{-6} \times 50 \times 5000 \text{ ps/m} = 105 \text{ ps}$$

The total delay change  $D_T = D_{UG} + D_{SF}$  will be less than 363 ps. We currently use a VOPS with 600 ps as the compensation delay line. The VOPS easily compensates the temperature change of more than 50 deg C and, when the control loop is closed, should keep the antenna links continually compensated for long periods of time.

### C. Photonic Link Reliability

The semiconductor laser diode life is about 200,000 hours (23 years). This mean-time-to fail is sufficient for a system with a single laser (such as a point-to-point system used in the telecommunication industry). However, an antenna array with 400 antennas can involve more than one thousand lasers per site. With an M/C service channel included, the number of required laser modules is even larger. Statistically, for a full-sized 400-antenna array complex, on average one laser module/transmitter will need to be replaced per week.

In the all-photonic link design, one HPLD laser located in the central control center may drive up to 16 antennas. This implies that  $\sim 25$  HPLDs are needed per DSCC, with an average failure rate of  $\sim 1$  HPLD per year. A “hot backup” HPLD laser could be implemented and connected to the main signal channel through a  $2 \times 1$  coupler and operated in parallel to the primary HPLD. The backup laser current can be set to run below the lasing threshold to extend its life and the output power of the prime HPLD monitored. If the primary HPLD output power drops below a preset level, the backup laser could be turned on but not put online. If the primary HPLD power falls below a second threshold, the backup HPLD could then be switched online.

### D. Wavelength Division Multiplexing

Wavelength division multiplexing (WDM) is a very efficient approach for high-capacity signal transmission and has been widely used in the telecommunication industry. A WDM system allows multiplexing of different wavelengths (up to hundreds of channels) through one single fiber. Each wavelength may carry up to a 40 Gb/s signal; therefore, one single optical fiber can carry signals to several terrabits per second (Tb/s, i.e.,  $10^{12}$  bits per second) or may carry several hundred channels of X-band signals. Note that in Fig. 1(a) the blocks labeled Opt Cpl are WDM couplers. In this design, we use three wavelengths passing through the main signal fiber  $f_{11}$  [up to  $f_{n1}$  in Fig. 1(a)]:  $\lambda_1$  and  $\lambda_2$  are used for RF signal modulation and transmission and  $\lambda_3$  for phase fluctuation detection and compensation. The laser diode labeled Cal TX in Fig. 1(a) transmits wavelength  $\lambda_3$ . This light signal is modulated by a calibration signal ( $\sim 400$  MHz) and sent out and back through the signal transport fiber  $f_{11}$ . The final received signal  $\lambda_3$  is demodulated at the calibration receiver (Cal RX) and compared with the original calibration reference signal. The resulting error signal is sent back to the VOPS to correct and compensate any phase change. Since both light  $\lambda_1$  and light  $\lambda_2$  are passed through the same fiber at different wavelengths, the system phase error will be correct without any channel (frequency) interference. In Fig. 1(a),  $\lambda_1$  is the X-band signal,  $\lambda_2$  is the Ka-band signal, and  $\lambda_3$  is the calibration signal.

### V. Initial Calibration Channel Tests

The integral calibration channel has been breadboarded and tested as shown schematically in Fig. 1(b). The resolution of the phase monitor has been measured to be  $< 1$  deg phase at X-band and  $\sim 3$  deg at Ka-band, sufficient to meet the array stabilization requirement. Initial open- and closed-loop operation of the signal transport stabilization circuit to an external thermal perturbation on a 2-km length of fiber-optic cable is shown in Figs. 3 through 5. With a perturbation of 3 deg C, the open-loop phase shift of  $\sim 400$  mV/deg C (Fig. 3) was reduced to  $\sim 1$  mV/deg C (Fig. 4) with the loop closed. This implies the transport link is stabilized at least a factor of 400 times. As can be seen in Fig. 5, the compensation factor may actually be higher and is currently limited to the precision of the phase measurement. The system electronic sensitivity to thermal and mechanical stress must still be determined to complete the feasibility demonstration of the stabilization approach, although a factor of 400 times is already similar to that achieved in the DSN SFODA systems [3–5].

Following complete characterization of the calibration channel, the X-band modulator will be integrated, which will allow demonstration of stabilized transport of received X-band signals. Characterization will then be extended to Ka-band signal transport.

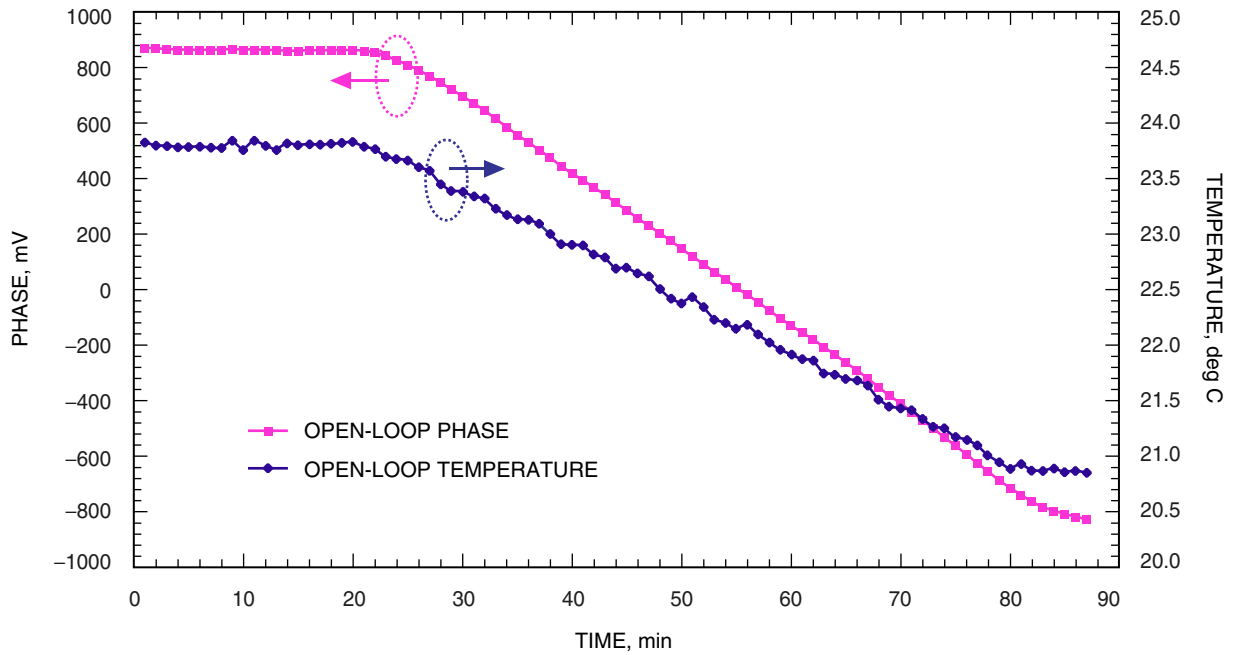


**Fig. 3. Calibration channel operating open loop: temperature change of 2-km distribution fiber-optic cable and corresponding phase change versus time.**

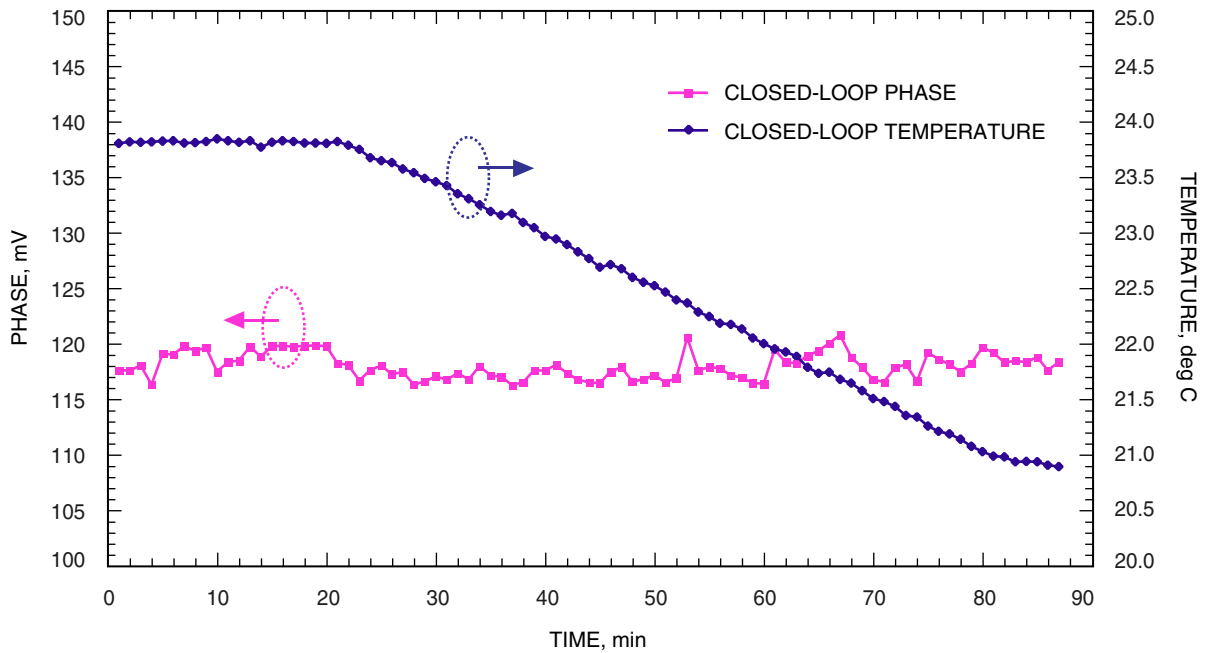


**Fig. 4. Calibration channel operating closed loop: temperature change of 2-km distribution fiber-optic cable and corresponding phase change versus time.**

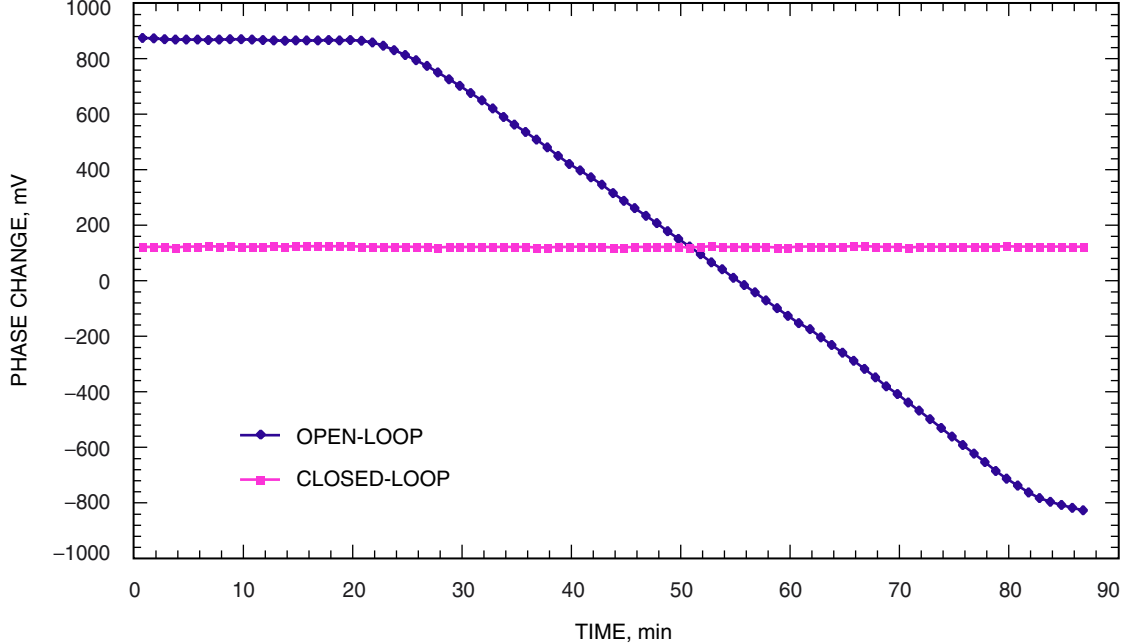


**Fig. 5. Comparison of the phase variation through a 2-km fiber-optic cable when the temperature has been changed 3 deg C when the loop is open and closed, demonstrating a stabilization of >400.**

## VI. Applicability to Uplink Arrays

A key challenge for the viability of replacing the DSN with a large array of antennas is the capability of the array to support uplink. Several uplink scenarios are presently under investigation, ranging from using a small number of large antennas (i.e., such as the 34-m antennas in the present DSN) to using a large array of very small antennas. There are multiple challenges with each scenario, but the primary consideration is that the phase of the transmitted signals from each antenna sum coherently at the receiving target. If uplink is accomplished using a very small number of antennas, existing techniques such as the FTS SFODA are still feasible. If the design includes a very large number of antennas, a lower cost stabilization approach such as described in this article becomes necessary.

Operationally, the two primary issues are how best to initially calibrate an array of antennas for a specific target and how to hold the calibration for long periods of uplink operation to avoid repeated recalibration. The error budget to phase align and stabilize transmitted signals to the receiving target has three major components: (1) local phase variations along the local signal path from the central transmitting source to each antenna, (2) variations due to the instantaneous and changing antenna geometry with respect to the moving spacecraft, and (3) variations in the atmosphere. The impact of temporal atmosphere variations depends on atmospheric cell size and the distance between the antennas. The effect of antenna geometry is in principle calculable, although knowledge and reproducibility of the phase center need to be confirmed. This development is directly applicable to (1) above and, with a means to provide closed-loop feedback control, the link can be continuously stabilized.

The distribution and stabilization concept for downlink arrays can also benefit uplink applications. One such uplink approach is schematically shown in Fig. 6. Only a single, central source X-band oscillator/synthesizer is required. The X-band signal to be transmitted is modulated onto the optical path originating from a single HPLD (in the uplink approach, only one modulator is required, rather than the one per antenna in the downlink approach). A lower-frequency ( $\sim 400$  MHz) calibration signal is also



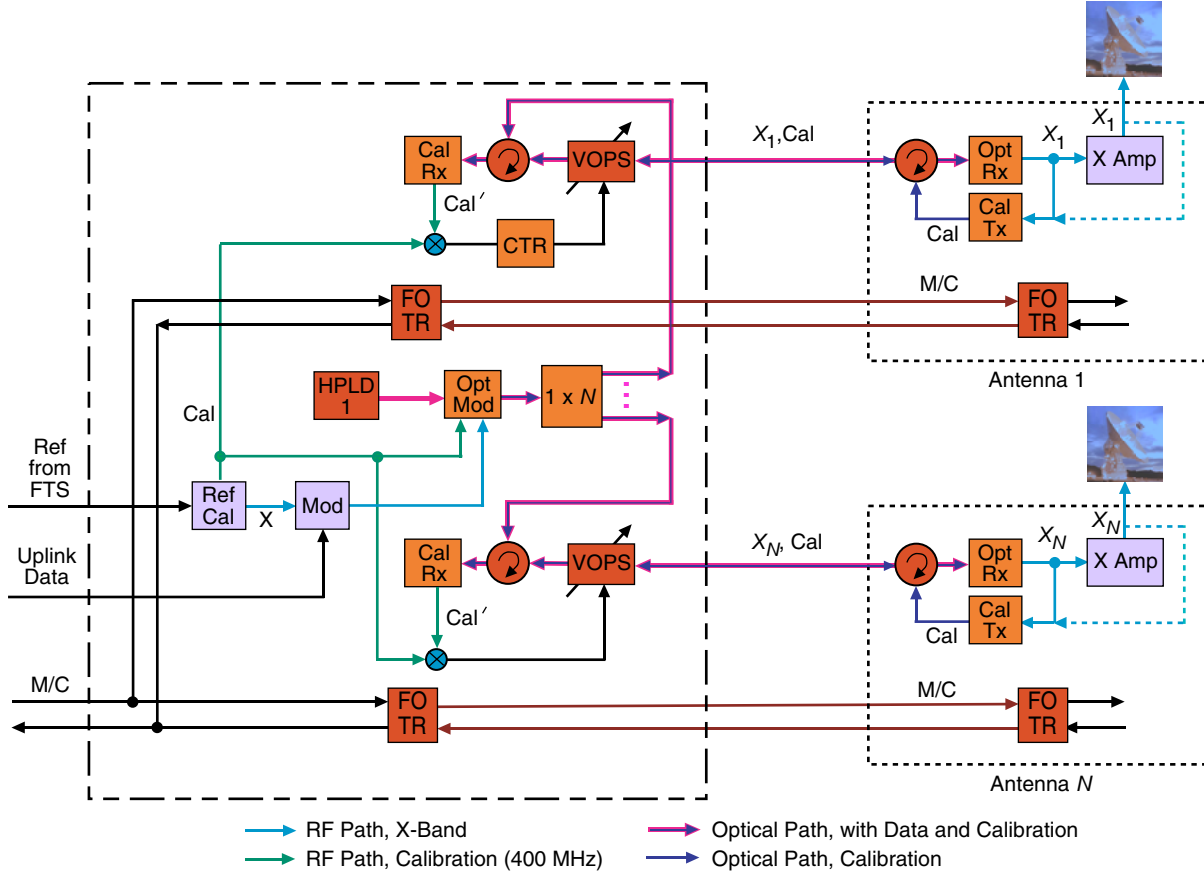


**Fig. 6. Conceptual block diagram of the stabilized “all-photonic link” features for uplink arrays ( $N$  antennas, X-band). For clarity, two antennas are shown.**

modulated onto the optical carrier. Both signals pass through a circulator and an optical phase shifter before traveling through the transport fiber to the antenna. Both signals are received by an optical receiver, where the X-band signal is amplified and transmitted to the spacecraft or uplink calibration target. The lower frequency calibration signal is retransmitted back down the transport fiber where the stabilization control loop is closed. While this scheme does require a low-cost optical transmitter at each antenna, the entire link is continually stabilized.

Ideally, the stabilized loop would account for phase variations all the way to the antenna phase center. In principle, the all-photonic link can be used to compensate for variations of the power amplifier as well. While the transmission link will be continually stabilized independently of the X-band signal transported up it, the inclusion of phase information measured at the output of the power amplifier (and ideally at the antenna phase center) could also be used, in principle, to control the VOPS. This feedback is schematically represented in Fig. 6 as a dashed line and would require a somewhat more expensive optical transmitter capable of transmitting an X-band feedback signal. This approach likely requires a discrete measurement and loop control method. If successful, it would significantly lengthen, and possibly eliminate, the need for ongoing array calibrations. The feasibility of this approach is not well known, but the potential benefit may warrant further study.

## VII. Conclusion

A development effort to design, develop, demonstrate, and evaluate a cost-effective “all-photonic” antenna link architecture providing stabilized broadband signal transport from near baseband to Ka-band was reported. The approach modulates RF signals directly onto an optical carrier that is derived from a central high-power laser transmitter. This photonic architecture eliminates all RF downconversion at the antenna, eliminates the requirement for PLLs or multipliers, and allows for all signal processing to be performed at the signal processing center. An integrated, low-frequency, and low-cost calibration channel is passed through the same signal transport fiber and continuously compensates for distribution path-length changes that result from temperature fluctuations and/or mechanical disturbances.

The all-photonic link approach provides improved operational stability and reliability, and relaxes control and maintenance requirements at all antenna pedestals. This should significantly simplify needed electronics, environmental control, and maintenance at each antenna in downlink and uplink antenna array architectures. These simplifications should provide significant benefit in reducing initial and life-cycle array costs. Currently a low-cost calibration channel has been breadboarded and tested in the JPL Frequency Standards Test Laboratory (FSTL), and it demonstrated stabilization similar to the best state-of-the-art systems currently operating in the DSN. This should have direct applicability to future FTS distribution applications and antenna array downlink and uplink system designs.

## Acknowledgments

The authors thank M. Calhoun for useful discussions on photonic system design and M. Tu for testing some of the optical components.

## References

- [1] D. Bagri, “A Proposed Array System for the Deep Space Network,” *The Interplanetary Network Progress Report*, vol. 42-157, Jet Propulsion Laboratory, Pasadena, California, pp. 1–16, May 15, 2004.  
[http://ipnpr/progress\\_report/42-157/157J.pdf](http://ipnpr/progress_report/42-157/157J.pdf)
- [2] S. Huang, M. Calhoun, and R. L. Tjoelker, “Stabilized Photonic Links for Frequency and Time Transfer,” *Proceedings of the 2006 IEEE Frequency Control Symposium*, Miami, Florida, June 2006.
- [3] M. Calhoun, G. J. Dick, and R. T. Wang, “Frequency Transfer and Cleanup for Ultra-High Stability of Both Long and Short Times for Cassini Ka-Band Experiment,” 30th Annual Precise Time and Time Interval Applications and Planning Meeting (PTTI), Reston, Virginia, December 1998.
- [4] M. Calhoun, R. Sydnor, and W. Deiner, “A Stabilized 100-Megahertz and 1-Gigahertz Reference Frequency Distribution for Cassini Radio Science,” *The Interplanetary Network Progress Report 42-148, October–December 2001*, Jet Propulsion Laboratory, Pasadena, California, pp. 1–11, February 15, 2002.  
[http://ipnpr/progress\\_report/42-148/148L.pdf](http://ipnpr/progress_report/42-148/148L.pdf)

- [5] M. Calhoun, R. Wang, A. Kirk, G. J. Dick, and R. L. Tjoelker, “Stabilized Reference Frequency Distribution for Radio Science with the Cassini Spacecraft and the Deep Space Network,” 32nd Annual Precise Time and Time Interval (PTTI) Systems and Applications Meeting, Reston, Virginia, November 28–30, 2000.
- [6] W. Shieh, G. Lutes, S. Yao, L. Maleki, and J. Garnica, “Performance of a 12-Kilometer Photonic Link for X-Band Antenna Remoting in NASA’s Deep Space Network,” *The Telecommunications and Mission Operations Progress Report 42-138, April–June 1999*, Jet Propulsion Laboratory, Pasadena, California, pp. 1–8, August 15, 1999. [http://ipnpr/progress\\_report/42-138/138D.pdf](http://ipnpr/progress_report/42-138/138D.pdf)